Journal of Sound and Vibration (2000) **234**(5), 725–736
doi:10.1006/jsvi.1999.2970, available online at http://www.idealibrary.com on IDEAL®

VIBRATION ANALYSIS FOR FRAME STRUCTURES USING TRANSFER OF DYNAMIC STIFFNESS COEFFICIENT

D. H. Moon and M. S. Choi

Department of Control and Mechanical Engineering, Pukyong National University, Pusan, Republic of Korea

(*Received* 5 *October* 1998, *and in final form* 7 *June* 1999)

In this paper, the authors formulate a free and forced vibration analysis algorithm for frame structures using the transfer dynamic stiffness coefficient method. This method is based on the concept of the transfer of the dynamic stiffness coefficient which is related to the force and displacement vector at each node from the left end to the right end of the structure. Numerical results by the transfer dynamic stiffness coefficient method for a space frame structure are compared with results by the finite element method and experiment. The validity and the convenience of the transfer dynamic stiffness coefficient method in solving dynamic problems accurately are confirmed.

1. INTRODUCTION

Complex and large frame-type structures are frequently used in the design of bridges, towers, cranes, and aerospace structures. In general, in order to analyze these frame structures, the finite element method (FEM) has been used. However, the FEM is necessary to use a large amount of computer memory and take a computation time as it requires many degrees of freedom for solving dynamic problems accurately for these structures [1]. Therefore, many engineers have studied various methods [2–7] to overcome these disadvantages, as have the authors.

Moon (one of the authors), Sueoka and Kondou have developed the transfer influence coefficient method as a method of vibration analysis with high computational efficiency and a high level of computational accuracy, and have confirmed the effectiveness by applying it to various important engineering structures [8–10]. However, this method cannot be applicable to a beam structure having closed loops (the so-called Rahmen structure). And so Kondou *et al*. developed the transfer stiffness coefficient method by introducing the concept of the substructure synthesis method into the algorithm of the transfer influence coefficient method. They formulated the algorithm of free and forced vibration analyses by modelling a straight-line beam structure as a lumped mass system and confirmed the effectiveness of it [11].

In this paper, we suggest a new vibration analysis algorithm; the transfer dynamic stiffness coefficient method (TDSCM). This method is based on the concept of the transfer of the dynamic stiffness coefficient which is related to the force and displacement vectors at each node from the left end to the right end of the structure, and in TDSCM the member between each node in frame structure was basically regarded as the distributed mass system.

0022-460X/00/300725 + 12 $35.00/0

We use the relationship of state variables between each node of basic member by introducing the concept of spectral element of Doyle [5].

We formulate the vibration analysis algorithm for frame structures by TDSCM in this paper. And the validity of the present algorithm is demonstrated through computational results by the TDSCM and the FEM on a personal computer, and experimental results.

2. TRANSFER DYNAMIC STIFFNESS COEFFICIENT METHOD

2.1. MODELLING

In order to simplify a variety of frame structures which consist of continuous beam and base support elements (springs and dampers), we consider a structure as an analytical model, as shown in Figure 1.

The boundary conditions of the structure are considered as base support elements of the left and the right ends of the structure. For example, in the case of the free end, it is replaced by a spring constant of zero, and in the case of the fixed end, by a spring constant of ∞.

In this paper, a node is called the discontinuous point of the force vector, such as a contact point between members, an excited point of application of external force and both ends of the structure. We designate nodes as node(0,∗), node(1,∗), ..., node(n,∗) successively from the left end to the right end. The mark "∗" denotes all nodes in the Y–Z plane of Figure 1.

We consider the analytical model as a series of subsystems as shown in Figure 2. The ith subsystem consists of four ith horizontal members, four transverse members, and four base support elements. Members are modelled as a continuous straight beam with a constant cross-sectional area and base support elements consist of six springs and six viscous dampers.

It is convenient that the node is analytically divided into the left-hand side and the right-hand side. The left-hand side of node(i,∗) is the point of connection of the ith horizontal member and the ith transverse member, and the right-hand side of node(i,∗) is a point of connection of the $(i+1)$th horizontal member and the ith transverse member. We indicate quantities related with the left-hand side of node(i,∗) as the head mark " $-$ " on symbols, and the right-hand side of node(i,∗) without the head mark.

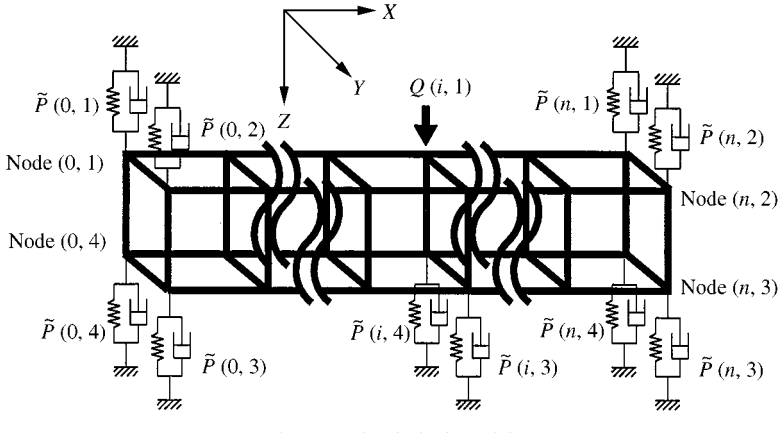

Figure 1. Analytical model.

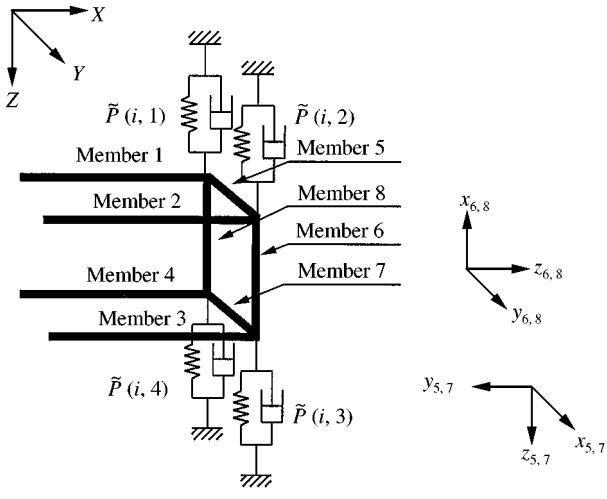

Figure 2. *I*th subsystem.

2.2. ELEMENT DYNAMIC STIFFNESS MATRIX

The exact element dynamic stiffness for the member can be found in many references [5, 7]. The element dynamic stiffness matrices $\mathbf{A}_i$, $\mathbf{B}_i$, $\mathbf{C}_i$, $\mathbf{D}_i$ of equation (1) catches the relationship between the force vectors $\mathbf{f}_i^{L,R} = {}^t\{F_x, M_x, F_y, M_z, F_z, M_y\}_i^{L,R}$ and the displacement vectors $\mathbf{u}_i^{L,R} = {}^t\{x, \theta_x, y, \theta_z, z, \theta_y\}_i^{L,R}$ of the left- and right-hand side of a continuous beam element in Figure 3 [5]. And the explicit form for the element dynamic stiffness matrix is given in Appendix A.

The subscript "i" indicates the quantity of the ith member or node(i,$*$) and the superscripts "L" and "R" express the quantity of the left- and right-hand side of the member:

$$\begin{bmatrix} \mathbf{f}_i^R \\ \mathbf{f}_i^L \end{bmatrix} = \begin{bmatrix} \mathbf{A}_i & \mathbf{B}_i \\ \mathbf{C}_i & \mathbf{D}_i \end{bmatrix} \begin{bmatrix} \mathbf{u}_i^R \\ \mathbf{u}_i^L \end{bmatrix}. \tag{1}$$

2.3. TRANSFER OF DYNAMIC STIFFNESS COEFFICIENT MATRIX

We define the relationship between force and displacement vector at left- and right-hand side of node(i,$*$) as follows:

$$\bar{\mathbf{F}}_i = \bar{\mathbf{S}}_i \mathbf{U}_i + \bar{\mathbf{E}}_i, \tag{2}$$

$$\mathbf{F}_i = \mathbf{S}_i \mathbf{U}_i + \mathbf{E}_i, \tag{3}$$

where $\bar{\mathbf{F}}_i$ and $\mathbf{F}_i$ are the total force vector at the left- and right-hand side of node(i,$*$), and $\mathbf{U}_i$ is the total displacement vector at node(i,$*$), where

$$\begin{aligned} \bar{\mathbf{F}}_i &= {}^t\{{}^t\bar{\mathbf{f}}_{(i,1)}, {}^t\bar{\mathbf{f}}_{(i,2)}, {}^t\bar{\mathbf{f}}_{(i,3)}, {}^t\bar{\mathbf{f}}_{(i,4)}\}, \\ \mathbf{F}_i &= {}^t\{{}^t\mathbf{f}_{(i,1)}, {}^t\mathbf{f}_{(i,2)}, {}^t\mathbf{f}_{(i,3)}, {}^t\mathbf{f}_{(i,4)}\}, \\ \mathbf{U}_i &= {}^t\{{}^t\mathbf{u}_{(i,1)}, {}^t\mathbf{u}_{(i,2)}, {}^t\mathbf{u}_{(i,3)}, {}^t\mathbf{u}_{(i,4)}\}. \end{aligned} \tag{4}$$

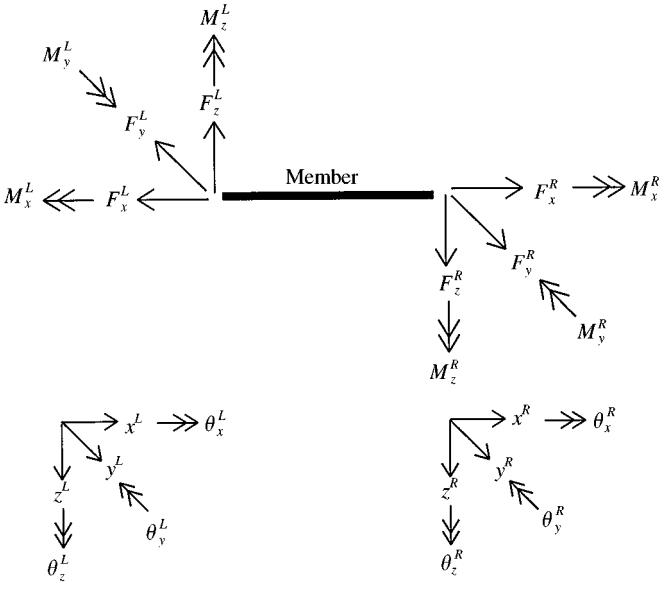

Figure 3. Definition of the direction of state variables.

We call $\bar{\mathbf{S}}_i$ and $\mathbf{S}_i$ as the dynamic stiffness coefficient matrices (24×24) of the left- and the right-hand side of the node(i,$*$) and $\bar{\mathbf{E}}_i$ and $\mathbf{E}_i$ as the force corrective vectors (24×1) of the left- and the right-hand side of node(i,$*$).

The relationship of the total force and displacement vectors at the right-hand side of node($i-1$,$*$) and at the left-hand side of node(i,$*$), applying equation (1) for each member, is the following:

$$\begin{bmatrix} \bar{\mathbf{F}}_i \\ \mathbf{F}_{i-1} \end{bmatrix} = \begin{bmatrix} \mathbf{A}_i^a & \mathbf{B}_i^a \\ \mathbf{C}_i^a & \mathbf{D}_i^a \end{bmatrix} \begin{bmatrix} \mathbf{U}_i \\ \mathbf{U}_{i-1} \end{bmatrix}, \tag{5}$$

where

$$\begin{aligned} \mathbf{A}_i^a &= \mathrm{diag}(\mathbf{A}_1, \mathbf{A}_2, \mathbf{A}_3, \mathbf{A}_4)_i, \\ \mathbf{B}_i^a &= \mathrm{diag}(\mathbf{B}_1, \mathbf{B}_2, \mathbf{B}_3, \mathbf{B}_4)_i, \\ \mathbf{C}_i^a &= \mathrm{diag}(\mathbf{C}_1, \mathbf{C}_2, \mathbf{C}_3, \mathbf{C}_4)_i, \\ \mathbf{D}_i^a &= \mathrm{diag}(\mathbf{D}_1, \mathbf{D}_2, \mathbf{D}_3, \mathbf{D}_4)_i. \end{aligned} \tag{6}$$

If we obtain the dynamic stiffness coefficient matrix $\mathbf{S}_{i-1}$ and the force corrective vector $\mathbf{E}_{i-1}$ of the right-hand side of node($i-1$,$*$), we can derive the dynamic stiffness coefficient matrix $\bar{\mathbf{S}}_i$ and the force corrective vector $\bar{\mathbf{E}}_i$ of the left-hand side of node(i,$*$) from equations (2), (5), and (3) into which $i = i - 1$ has been substituted as follows:

$$\begin{aligned} \bar{\mathbf{S}}_i &= \mathbf{A}_i^a + \mathbf{B}_i^a \mathbf{V}_i, \\ \bar{\mathbf{E}}_i &= -\mathbf{B}_i^a \mathbf{G}_i^{-1} \mathbf{E}_{i-1}, \end{aligned} \tag{7}$$

where

$$\mathbf{V}_i = \mathbf{G}_i^{-1}\mathbf{C}_i^a,$$

$$\mathbf{G}_i = \mathbf{S}_{i-1} - \mathbf{D}_i^a. \tag{8}$$

If node$(i, 1)$ is excited by harmonic external force $\mathbf{Q}_{(i,1)}$, the equilibrium equation of the dynamic force vector at node$(i, *)$ is the following:

$$\mathbf{F}_i = \bar{\mathbf{F}}_i + \mathbf{P}_i\mathbf{U}_i - \mathbf{Q}_i, \tag{9}$$

where matrix $\mathbf{P}_i$ and vector $\mathbf{Q}_i$ are given as

$$\mathbf{P}_i = \check{\mathbf{P}}_i + \hat{\mathbf{P}}_i,$$

$$\check{\mathbf{P}}_i = \mathrm{diag}(\tilde{\mathbf{P}}_{(i,1)}, \tilde{\mathbf{P}}_{(i,2)}, \tilde{\mathbf{P}}_{(i,3)}, \tilde{\mathbf{P}}_{(i,4)}),$$

$$\tilde{\mathbf{P}}_{(i,*)} = \mathrm{diag}(k_x + \mathrm{j}c_x\omega, K_x + \mathrm{j}C_x\omega, k_y + \mathrm{j}c_y\omega, K_z + \mathrm{j}C_z\omega, k_z + \mathrm{j}c_z\omega, K_y + \mathrm{j}C_y\omega)_{(i,*)},$$

$$\hat{\mathbf{P}}_i = \begin{bmatrix} \hat{\mathbf{D}}_5 + \hat{\mathbf{A}}_8 & \hat{\mathbf{C}}_5 & \mathbf{0} & \hat{\mathbf{B}}_8 \\ \hat{\mathbf{B}}_5 & \hat{\mathbf{A}}_5 + \hat{\mathbf{A}}_6 & \hat{\mathbf{B}}_6 & \mathbf{0} \\ \mathbf{0} & \hat{\mathbf{C}}_6 & \hat{\mathbf{D}}_6 + \hat{\mathbf{A}}_7 & \hat{\mathbf{B}}_7 \\ \hat{\mathbf{C}}_8 & \mathbf{0} & \hat{\mathbf{C}}_7 & \hat{\mathbf{D}}_7 + \hat{\mathbf{D}}_8 \end{bmatrix},$$

$$\hat{\mathbf{A}}_{5,7} = \mathbf{R}\mathbf{A}_{5,7}\,{}^t\mathbf{R}, \qquad \hat{\mathbf{B}}_{5,7} = \mathbf{R}\mathbf{B}_{5,7}\,{}^t\mathbf{R},$$

$$\hat{\mathbf{C}}_{5,7} = \mathbf{R}\mathbf{C}_{5,7}\,{}^t\mathbf{R}, \qquad \hat{\mathbf{D}}_{5,7} = \mathbf{R}\mathbf{D}_{5,7}\,{}^t\mathbf{R},$$

$$\hat{\mathbf{A}}_{6,8} = \mathbf{R}'\mathbf{A}_{6,8}\,{}^t\mathbf{R}', \qquad \hat{\mathbf{B}}_{6,8} = \mathbf{R}'\mathbf{B}_{6,8}\,{}^t\mathbf{R}',$$

$$\hat{\mathbf{C}}_{6,8} = \mathbf{R}'\mathbf{C}_{6,8}\,{}^t\mathbf{R}', \qquad \hat{\mathbf{D}}_{6,8} = \mathbf{R}'\mathbf{D}_{6,8}\,{}^t\mathbf{R}',$$

$$\mathbf{Q}_i = {}^t({}^t\mathbf{Q}_{(i,1)}, {}^t\mathbf{0}, {}^t\mathbf{0}, {}^t\mathbf{0}), \tag{10}$$

where $\mathbf{R}$ and $\mathbf{R}'$ are matrices which transform local co-ordinates of transverse members 5, 7 and 6, 8 into the global co-ordinates, and $(\mathbf{A}, \mathbf{B}, \mathbf{C}, \mathbf{D})_{5,6,7,8}$ are submatrices of the element dynamic stiffness matrix of transverse members 5, 6, 7 and 8.

We can derive the dynamic stiffness coefficient matrix $\mathbf{S}_i$ and the force corrective vector $\mathbf{E}_i$ at the right-hand side of node$(i,*)$ from equations (2), (3), and (9):

$$\mathbf{S}_i = \bar{\mathbf{S}}_i + \mathbf{P}_i,$$

$$\mathbf{E}_i = \bar{\mathbf{E}}_i - \mathbf{Q}_i. \tag{11}$$

Therefore, if we take the dynamic stiffness coefficient matrix $\mathbf{S}_{i-1}$ and the force corrective vector $\mathbf{E}_{i-1}$ at the right-hand side of node$(i-1,*)$, we can obtain the dynamic stiffness coefficient matrix $\mathbf{S}_i$ and the force corrective vector $\mathbf{E}_i$ at the right-hand side of node$(i,*)$, from equations (7), (11) are as follows:

$$\begin{aligned} \mathbf{S}_i &= \mathbf{A}_i^a + \mathbf{B}_i^a\mathbf{V}_i + \mathbf{P}_i \\ \mathbf{E}_i &= -\mathbf{B}_i^a\mathbf{G}_i^{-1}\mathbf{E}_{i-1} - \mathbf{Q}_i \end{aligned} \qquad (i = 1, 2, \ldots, n). \tag{12}$$

Because the boundary condition of the left end is modelled as the base support element at node(0,∗), force vector $\bar{\mathbf{F}}_0$ at the left-hand side of node(0,∗) is a null vector. We can find matrix $\mathbf{S}_0$ and vector $\mathbf{E}_0$ from the equilibrium equation of the force vector at node(0,∗) and equation (3) into which $i = 0$ has been substituted as follows:

$$\mathbf{S}_0 = \mathbf{P}_0, \qquad \mathbf{E}_0 = -\mathbf{Q}_0. \tag{13}$$

Next, matrix $\mathbf{S}_i$ and vector $\mathbf{E}_i$ at node(i,∗) are computed from equations (12) and (13) for $i = 1, 2, \ldots, n$. Finally, we can find the dynamic stiffness coefficient matrix $\mathbf{S}_n$ and the force corrective vector $\mathbf{E}_n$ of the right-hand side of node(n,∗), that is, the right end of the structure.

2.4. FORCED VIBRATION ANALYSIS

Because we consider the boundary condition of the right end of the structure as the base support element of node(n,∗), the right-hand side of node(n,∗) can be considered as being analytically free, that is, $\mathbf{F}_n = \mathbf{0}$, $\mathbf{U}_n \neq \mathbf{0}$. From $\mathbf{F}_n = \mathbf{0}$ and equation (3) into which $i = n$ has been substituted, $\mathbf{U}_n$ is obtained as

$$\mathbf{U}_n = -\mathbf{S}_n^{-1}\mathbf{E}_n. \tag{14}$$

The displacement vectors $\mathbf{U}_{n-1}, \mathbf{U}_{n-2}, \ldots, \mathbf{U}_0$ are computed from equations (3), (5) and (8) as follows:

$$\mathbf{U}_{i-1} = \mathbf{V}_i\mathbf{U}_i - \mathbf{G}_i^{-1}\mathbf{E}_{i-1} \quad (i = n, n-1, \ldots, 1). \tag{15}$$

If $\mathbf{U}_i$ is known, $\bar{\mathbf{F}}_i$ ($i = 1, 2, \ldots, n$) and $\mathbf{F}_i$ ($i = 0, 1, \ldots, n-1$) are computed from equations (2) and (3).

2.5. FREE VIBRATION ANALYSIS

In free vibration analysis, it is not necessary to transfer the force corrective vector; only the transfer of the dynamic stiffness coefficient matrix is required. As the right-hand side of node(n,∗) can be considered analytically as being free, that is, $\mathbf{F}_n = \mathbf{0}$, $\mathbf{U}_n \neq \mathbf{0}$.

From $\mathbf{F}_n = \mathbf{0}$, $\mathbf{U}_n \neq \mathbf{0}$ and equation (3) excepting the force corrective vector term for $i = n$, the frequency equation is as follows:

$$\det \mathbf{S}_n = 0. \tag{16}$$

We can obtain the natural frequency from equation (16) and matrix $\mathbf{S}_n$ of equation (16) is computed through equation (12). In computation process of matrix $\mathbf{S}_i$ of equation (12), we have to find the inverse matrix of $\mathbf{G}_i$. In this case, if the determinant of matrix $\mathbf{G}_i$ is zero, elements of matrix $\mathbf{S}_i$ become usually asymmetric poles that change their sign before and after the poles of elements. It may not be easy to compute matrix $\mathbf{S}_{i+1}$ of node $i + 1$ by equation (12). Therefore, elements of matrix $\mathbf{S}_n$ may contain the asymmetric poles and then numerical instability may occur in computation process of the frequency equation (16). As a result, we may obtain the false roots (asymmetric poles) as the true roots (natural frequencies). These false roots must be eliminated by applying the following technique as described in the previous report [8, 9]. This technique introduces the sign function to eliminate the asymmetric pole which may occur in solving equation (12) at each node.

The sign function Z of equation (17) means that the asymmetric poles are all transformed into symmetric poles by multiplying $\mathrm{sgn}(\det \mathbf{S}_n)$ by the sign functions of $\mathrm{sgn}(\det \mathbf{G}_i)$ $(i = 1, 2, 3, \ldots, n)$.

$$Z = \prod_{i=1}^{n} \mathrm{sgn}(\det \mathbf{G}_i)\, \mathrm{sgn}(\det \mathbf{S}_n). \tag{17}$$

Consequently, we obtain only the true roots by applying the bisection method to equation (17), as the bisection method necessitates only the sign of the value of the function. Because the natural frequency of the structure is generally a single root, the zeros (natural frequencies) of equation (16) are assumed to be zero points of the first order. We cannot find a few natural frequencies when two roots are very close to each other, but these are obtained by varying the natural frequency in small steps.

The characteristic modes are computed from the right end to the left end successively using equation (18) after the displacement vector of node$(n,*)$ has been obtained:

$$\mathbf{U}_{i-1} = \mathbf{V}_i \mathbf{U}_i. \tag{18}$$

3. NUMERICAL EXAMPLES AND DISCUSSION

We used MATLAB language in programming and computed natural frequencies and frequency–responses for the computational model of Figure 4 on a personal computer. In order to compare with the other method, we carried out the same computation by using the NISA II [12], which is based on the FEM.

The data for all members of the frame structure in Figure 4 are given in Table 1. Table 2 indicates the natural frequencies for the computational model by using the FEM, the TDSCM, and experiment. Parentheses in the table show the size of the matrix needed to solve eigenvalues problem on the FEM, and the size of matrix $\mathbf{S}_n$ to solve the frequency

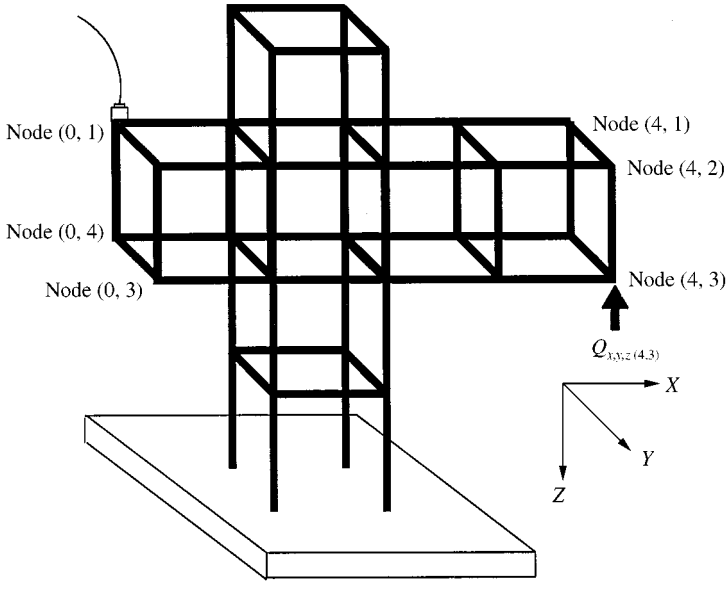

Figure 4. Computational model.

TABLE 1

Computational model data

Length of member element (l)	250 mm
Width of member element	10 mm
Thickness of member element	10 mm
Mass density (ρ)	$7{\cdot}69474 \times 10^3$ kg/m^3
Young's modulus (E)	$2{\cdot}06 \times 10^{11}$ N/m
Shear modulus (G)	$7{\cdot}9231 \times 10^{10}$ N/m
The Poisson ratio (v)	0·3

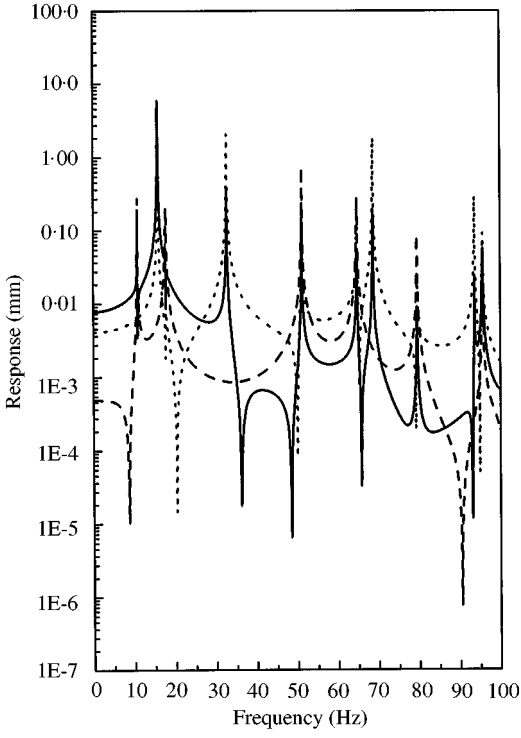

Figure 5. Frequency–response of computational model by TDSCM: —, X; – – –, Y; - - - -, Z.

equation on the TDSCM. The experiment was carried out by using an FFT analyzer, an impact hammer and a triaxial accelerometer.

We confirmed that the results of the FEM II (504 DOFs), better than those of the FEM I (144 DOFs), approximately agreed with those of the TDSCM. It is the reason why the TDSCM is modelled by a continuous system, and the FEM by a discrete system. And the FEM II has the matrix size of 504×504 in solving the eigenvalue problem for the present model in limit frequency region. On the other hand, if we use the TDSCM, the matrix size of the dynamic stiffness coefficient matrix $\mathbf{S}_n$ is only 24×24. Therefore, the TDSCM is superior to the FEM in computational efficiency owing to saving of computation time and using memory of computer in the case of solving the dynamic problem for complex and large structures on a personal computer.

When the harmonic external force is given to Z direction at node(4,3) in Figure 4, Figure 5 shows the frequency–response curves of X, Y and Z directions at node(0,1) by using the TDSCM. The amplitude of the harmonic external force is 1 N and the forced frequencies are 0·1, 0·2, …, 100 Hz. The resonant frequencies of the frequency–response curves using the TDSCM coincide with the natural frequencies of Table 2.

Table 3 indicates the frequency–response of Y direction at node(0,1) in Figure 4 using the FEM and the TDSCM. The excited frequencies are 1, 10, 20, …, 100 Hz. The results of the FEM⟨50⟩, which are computed with 1st–50th natural modes of the FEM II, rather than those of the FEM⟨10⟩ with 1st–10th natural modes, are very similar to those of the TDSCM. We confirmed that the results of the FEM which consider many natural modes approximate to those of the TDSCM. However, we already confirmed in the FEM I of Table 2 that the results of the FEM are not accurate in finding the high natural frequencies.

TABLE 2

Comparison of natural frequencies for computational model (*Hz*)

Order	FEM I (144 × 144)	FEM II (504 × 504)	TDSCM (24 × 24)	Experiment
1	10·811	10·810	10·809	10·9
2	15·812	15·811	15·811	15·6
3	17·752	17·750	17·750	17·6
4	32·731	32·721	32·721	32·5
5	51·216	51·186	51·183	50·4
6	64·814	64·742	64·738	65·1
7	68·771	68·686	68·683	68·3
8	79·673	79·540	79·535	79·7
9	93·891	93·687	93·677	94·0
10	95·845	95·669	95·658	96·4
20	164·54	163·72	163·66	164·5
30	421·15	380·33	379·16	—
40	487·49	426·89	425·05	—
50	620·38	510·66	507·48	—

TABLE 3

Comparison of frequency–responses for computational model (*mm*)

Frequency	FEM⟨10⟩	FEM⟨50⟩	TDSCM
1	4·540E − 4	4·865E − 4	4·866E − 4
10	1·775E − 3	1·743E − 3	1·747E − 3
20	4·410E − 3	4·376E − 3	4·376E − 3
30	9·690E − 4	9·341E − 4	9·340E − 4
40	1·057E − 3	1·020E − 3	1·020E − 3
50	9·763E − 3	9·723E − 3	9·744E − 3
60	3·241E − 3	3·285E − 3	3·286E − 3
70	1·807E − 3	1·757E − 3	1·755E − 3
80	6·120E − 3	6·177E − 3	6·103E − 3
90	4·181E − 5	2·161E − 5	2·183E − 5
100	2·189E − 4	1·826E − 4	1·812E − 4

Therefore, it is very difficult for a person who is not a specialist in the FEM to select a suitable partition number of members for accurate eigenvalue analysis and a suitable number of modes for frequency–response analysis. On the other hand, if one uses the TDSCM for vibration analysis of complex and large frame structures, it is very simple to solve dynamic problems accurately.

4. CONCLUSION

The authors formulated a free and forced vibration analysis algorithm for frame structures using the transfer dynamic stiffness coefficient method.

Numerical results for the frame structure by the transfer dynamic stiffness coefficient method on a personal computer were compared with results by the finite element method and experimental results. As a result, the validity and the convenience of the transfer dynamic stiffness coefficient method in solving dynamic problems of complex and large frame structures accurately were confirmed.

REFERENCES

1. N. S. SEHMI 1989 *Large Order Structural Eigenanalysis Techniques Algorithm for Finite Element Systems*. New York: Ellis Horwood Limited Publishers.
2. EDUARD C. PESTEL and FREDERICK A. LECKIE 1963 *Matrix Methods in Elastomechanics*. New York: McGraw-Hill Publishers.
3. M. A. DOKAINISH 1972 *ASME Journal of Engineering for Industry* **94**, 526–530. A new approach for plate vibration: combination of transfer matrix and finite-element technique.
4. M. OHGA, T. SHIGEMATSU and T. HARA 1983 *Computers and Structures* **17**, 321–326. Structural analysis by a combined finite element-transfer matrix method.
5. JAMES F. DOYLE 1991 *Static and Dynamic Analysis of Structures with An Emphasis on Mechanics and Computer Matrix Methods*. London: Kluwer Academic Publishers.
6. B. S. YANG and W. D. PILKEY 1992 *Machine Vibration* **1**, 164–170. Accurate approach to free vibration analysis for a rotating shaft.
7. M. GERADIN and S. L. CHEN 1995 *Journal of Sound and Vibration* **185**, 431–440. An exact model reduction technique for beam structures: combination of transfer and dynamic stiffness matrices.
8. T. KONDOU, A. SUEOKA, K. YAMASHITA, D. H. MOON and T. KAWAMURA 1991 *JSME International Journal Series III* **34**, 33–41. Free vibration analysis of a multiple straight-line structure regarded as a distributed mass system by the transfer influence coefficient method.
9. T. KONDOU, A. SUEOKA, Y. YASUDA and D. H. MOON 1992 *JSME International Journal Series III* **35**, 22–31. Free vibration analysis of a tree structure by the transfer influence coefficient method (1st Report, Formulation for a two-dimensional tree structure).
10. T. KONDOU, A. SUEOKA, Y. YASUDA and D. H. MOON 1992 *JSME International Journal Series III* **35**, 32–40. Free vibration analysis of a tree structure by the transfer influence coefficient method (2nd Report, Treatment of a three-dimensional tree structure and numerical computational results).
11. T. KONDOU, T. AYABE and A. SUEOKA 1996 *Transactions of the Japan Society of Mechanical Engineering*(*C*) **62**, 1277–1284. Transfer stiffness coefficient method combined with the concept of substructure synthesis method (Linear free and forced vibration analyses of a straight-line beam structure).
12. ENGINEERING MECHANICS RESEARCH CORPORATION 1993 *User's Manual for NISA II*.

APPENDIX A

If a member is modelled as a Euler beam, the submatrices **A**, **B**, **C**, **D** are as follows:

$$\mathbf{A} = \mathrm{diag}(A_{11}, A_{22}, \mathbf{A}', \mathbf{A}'),$$
$$\mathbf{B} = \mathrm{diag}(B_{11}, B_{22}, \mathbf{B}', \mathbf{B}'),$$
$$\mathbf{C} = \mathrm{diag}(C_{11}, C_{22}, \mathbf{C}', \mathbf{C}'),$$
$$\mathbf{D} = \mathrm{diag}(D_{11}, D_{22}, \mathbf{D}', \mathbf{D}').$$

The longitudinal dynamic stiffnesses $A_{11}, B_{11}, C_{11}, D_{11}$ are given as

$$A_{11} = \frac{E'A\delta}{l\sin\delta}\cos\delta = -D_{11},$$
$$B_{11} = -\frac{E'A\delta}{l\sin\delta} = -C_{11},$$
$$\delta = l\omega\sqrt{\frac{\mu}{E'A}}.$$

The torsional dynamic stiffnesses $A_{22}, B_{22}, C_{22}, D_{22}$ are expressed as

$$A_{22} = \frac{G'I_p\beta_t}{l\sin\beta_t}\cos\beta_t = -D_{22},$$
$$B_{22} = -\frac{G'I_p\beta_t}{l\sin\beta_t} = -C_{22},$$
$$\beta_t = l\omega\sqrt{\frac{\mu l}{G'A}}.$$

The bending dynamic stiffness matrices $\mathbf{A}', \mathbf{B}', \mathbf{C}', \mathbf{D}'$ are as follows:

$$\mathbf{A}' = \begin{bmatrix} A'_{11} & A'_{12} \\ A'_{21} & A'_{22} \end{bmatrix}, \qquad \mathbf{B}' = \begin{bmatrix} B'_{11} & B'_{12} \\ B'_{21} & B'_{22} \end{bmatrix},$$

$$\mathbf{C}' = \begin{bmatrix} C'_{11} & C'_{12} \\ C'_{21} & C'_{22} \end{bmatrix}, \qquad \mathbf{D}' = \begin{bmatrix} D'_{11} & D'_{12} \\ D'_{21} & D'_{22} \end{bmatrix},$$

$$A'_{11} = \frac{E'I}{l^3}(\alpha) = -D'_{11},$$
$$A'_{12} = \frac{E'I}{l^3}(-\bar{\gamma}l) = A'_{21} = D'_{12} = D'_{21},$$
$$A'_{22} = \frac{E'I}{l^3}(\beta l^2) = -D'_{22},$$
$$B'_{11} = \frac{E'I}{l^3}(-\bar{\alpha}) = -C'_{11},$$
$$B'_{12} = \frac{E'I}{l^3}(-\gamma l) = -B'_{21} = C'_{12} = -C'_{21},$$
$$B'_{22} = \frac{E'I}{l^3}(\bar{\beta}l^2) = -C'_{22},$$

$$\alpha = (\cos\varepsilon \sinh\varepsilon + \sin\varepsilon \cosh\varepsilon)\,\varepsilon^3/ddet,$$
$$\bar{\alpha} = (\sin\varepsilon + \sinh\varepsilon)\,\varepsilon^3/ddet,$$
$$\beta = (-\cos\varepsilon \sinh\varepsilon + \sin\varepsilon \cosh\varepsilon)\,\varepsilon/ddet,$$
$$\bar{\beta} = (-\sin\varepsilon + \sinh\varepsilon)\,\varepsilon/ddet,$$
$$\gamma = (-\cos\varepsilon + \cosh\varepsilon)\,\varepsilon^2/ddet,$$
$$\bar{\gamma} = (\sin\varepsilon \sinh\varepsilon)\,\varepsilon^2/ddet,$$
$$ddet = (1 - \cos\varepsilon \cosh\varepsilon), \quad \varepsilon = l\sqrt{\omega\ \sqrt{\frac{\mu}{E'I}}},$$
$$G' = E'/2(1+\nu), \quad E' = E(1 + j\eta),$$

where ω is the natural angular frequency, l is the length of a member, μ is the linear density, A is the cross-sectional area, I is the moment of inertia, I_p is the polar moment of inertia, G is the shear modulus, ν is the Poisson ratio, E is the Young's modulus, η is the structural damping coefficient, $E'(G')$ is the complex Young's (shear) modulus.